ISSN 1063-7834, Physics of the Solid State, 2012, Vol. 54, No. 11, pp. 2243–2252. © Pleiades Publishing, Ltd., 2012.
Original Russian Text © A.P. Levanyuk, I.B. Misirlioglu, E.D. Mishina, A.S. Sigov, 2012, published in Fizika Tverdogo Tela, 2012, Vol. 54, No. 11, pp. 2106–2114.

FERROELECTRICITY

Effects of the Depolarization Field in a Perforated Film of the Biaxial Ferroelectric

A. P. Levanyuk[a, b], I. B. Misirlioglu[c], E. D. Mishina[a, *], and A. S. Sigov[a]

[a] *Moscow State Technical University of Radio-Engineering, Electronics and Automation, pr. Vernadskogo 78, Moscow, 117454 Russia*

** e-mail: mishina_elena57@mail.ru*

[b] *Departamento de Fisica de la Materia Condensada, Universidad Autonoma de Madrid, Ciudad Universitaria de Cantoblanco, Madrid, 28049 Spain*

[c] *Faculty of Engineering and Natural Sciences, Sabanci University, Orhanli–Tuzla, Istanbul, 34956 Turkey*

Received March 5, 2012

Abstract—The domain structure in a biaxial ferroelectric layer perforated by cylindrical channels has been investigated using the numerical simulation based on the phenomenological theory of ferroelectricity and the equations of electrostatics in the framework of the Gauss–Seidel iterative method. Both polar axes lie in the plane of the film, which is characteristic of thin epitaxial films of $BaTiO_3$ and $(Ba_{1-x}Sr_x)TiO_3$ on a MgO substrate. The calculations have been performed using the parameters of $BaTiO_3$, which does not matter because of the qualitative character of the results: the electrostatic problem is two-dimensional and formally applies to infinitely thick layers rather than to thin layers. The primary attention has been paid to the systems containing sixteen channels. Two different orientations of the polar axes with respect to the lattice channels have been considered. It has been shown that, for these orientations, the domain structure has a different character: when the line with the minimum distance between the channels is perpendicular to the bisector of the angle between the polar axes, this structure contains a single channel in the repeating motif and a polarization vortex; when one of the polar axes is perpendicular to the line with the minimum distance between the channels, the situation is less clear. There are indications that the repeating motif of the domain structure in a system of many channels contains two channels and does not contain vortices. The strong influence of the electrodes on the domain structure in this case has been noted.

DOI: 10.1134/S1063783412110170

1. INTRODUCTION

Photonic crystals based on ferroelectric materials have attracted the particular attention of many researchers. One of the possibilities to create a switchable two-dimensional photonic crystal is that a ferroelectric with the spontaneous polarization vector lying in the plane of the film is used as the main optical material. A photonic crystal can be fabricated, for example, by means of the perforation of a film in such a way as to obtain a two-dimensional lattice of holes. Experiments of this type were performed and described in our previous works [1, 2]. More specifically, we studied $(Ba_{0.8}Sr_{0.2})TiO_3$ epitaxial films on a MgO substrate, which were perforated by a focused ion beam. This process resulted in the formation of a two-dimensional lattice of holes with a diameter of 300 nm and a period of 450 nm. The properties of the photonic crystal thus fabricated proved to be very promising, on the one hand, and not entirely understood, on the other hand. This contradiction has motivated us to perform a theoretical analysis of the phenomena that can be expected to occur in such systems. In this work, we have investigated domain structures that are related to the expected structures in perforated thin films of a biaxial ferroelectric in the case where the two polar axes lie in the plane of the film. According to [3], it is this situation that takes place in $(Ba_{0.8}Sr_{0.2})TiO_3$ films on MgO substrates with thicknesses smaller than 20 nm. To the best of our knowledge, experimental data for such films are not available in the literature. In [1, 2], we studied films of the above composition with a larger thickness (approximately 70 nm); therefore, the case in point is not an interpretation of the experimental results [1, 2] on the basis of the theoretical conclusions drawn in the present work.

We should emphasize that, even if such data were to be available, it would be impossible to perform a direct comparison between theory and experiment at this stage of investigations because of the complexity of the expected domain structure and its dependence on many factors (including those uncontrollable now), as well as by virtue of the illustrative character of the theory. The complexity of the domain structure is associated with the fact that inhomogeneities of the polarization lying in the plane of the film can induce a strong depolarization field, which has a long-range character and, hence, in turn, affects the polarization over a wide range. Even for a nonuniform polarization lying entirely in the plane of the thin film, the generated depolarization field is three-dimensional, which greatly complicates the calculations; consequently, we have to ignore this circumstance. Therefore, our "two-dimensional" calculation applies not to thin films but to infinitely thick layers that are perforated by very long cylindrical channels. This perforation is common that exists in both the thick and thin films. The effects of perforation are considerably simpler in thick layers. To the best of our knowledge, these effects have not been investigated previously; therefore, we begin our consideration precisely with this case. It is hoped that the qualitative character of the results will remain the same for thin films, although, of course, this is not entirely obvious and deserves a separate investigation.

It should be noted that, at present, the changeover to the case of thin films would be premature, because there are a number of problems that remain unsolved even in the simpler case of thick layers, for example, the problem of sensitivity of a depolarization field to variations in the conditions of its screening on the surface of the holes. Some studies have clearly demonstrated the efficiency of the screening of a depolarization field by means of the adsorption of ions on the surface of ferroelectric films [4]. We are unaware of the occurrence and, especially, the specific features of this screening on the surface of the holes obtained by ion beam etching. Before investigating the aforementioned problem, it would be helpful to understand the qualitative features of this effect even though for thick layers. Another important factor is associated with the effects of solid-state elasticity, which are often responsible for the possible orientations of the domain walls. It is also of interest to investigate the evolution of the domain structure upon application of an external electric field, including the switching of the spontaneous polarization. All these problems, which are eventually of interest for thin films, should be solved, in our opinion, first of all for thick layers.

Since the analytical approach even to the two-dimensional problem is not practical, the basic method used for obtaining the results in the present study is the numerical solution of the equation of state of a ferroelectric in combination with the equations of electrostatics. The application of this method to large-sized systems involves considerable computational difficulties, the overcoming of which is hardly reasonable at the present time in view of the aforementioned features. Therefore, we have investigated the system with holes whose diameter is considerably smaller than that in the above experiments. The changeover to larger sizes is another possible direction of the future investigation.

In works similar to our study, it is natural to begin the analysis with the consideration of simplest systems in which the regularities responsible for the formation of domain structures are especially well pronounced. We begin our investigation with the consideration of square pellets (columns) with one hole (channel). Already at this stage, by artificially introducing the periodic boundary conditions, we will attempt to identify equilibrium domain structures expected in large-sized systems. At the next stage, we will investigate the domain structures in the system with sixteen channels. We are interested in the effects exerted by the depolarization fields of the channels rather than in those of the external surfaces of the prismatic column. For this purpose, we use only two types of electrostatic boundary conditions at the interfaces of the system: (i) the specified electrical potential, which physically corresponds to the metallization of the system; and (ii) the periodic boundary conditions in order to elucidate the behavior of large-sized systems. Since we take into account the polarization gradients in the equations of state, it is necessary to specify additional boundary conditions for the polarization. In order to identify exactly the electrostatic effects, the surface is considered to be neutral with respect to the polarization. This means that the derivatives of the components of the polarization along the normal to the surface are equal to zero (infinity of the so-called extrapolation length) and that the polarity of the surface itself is ignored. In the numerical calculations, we use the parameters of the ideal $BaTiO_3$ epitaxial films on the MgO substrate.

2. FORMULATION OF THE PROBLEM AND METHOD OF INVESTIGATION

Let us consider a column in the form of a cylinder surrounded by vacuum. The material of the column is a biaxial ferroelectric with the polar axes perpendicular to the axis of the cylinder. The phase transition to a single-domain state in this system is not possible because of the significant value of the depolarization field. For an infinite cylinder polarized perpendicular to the cylinder axis, the depolarization field has the form

$$E_{\text{dep}} = -\frac{P}{2\varepsilon_0}. \quad (1)$$

After substituting this expression into the equation of state of the ferroelectric

$$AP + BP^3 = E, \quad (2)$$

where it is sufficient to take into account only one component of the polarization, we obtain

$$\left(A + \frac{1}{2\varepsilon_0}\right)P + BP^3 = 0. \quad (3)$$

This equation always gives the result $P = 0$, because the expression in the parentheses is always positive owing to the large value of the second term.

It is natural to expect, therefore, that the distribution of the polarization observed in such a cylinder due to the phase transition will have the form of a vortex.

However, in this case, no electric field is generated, which is well known, for example, for magnetic materials. The magnetic vortices and other zero-field domain structures ("structures with a closed magnetic flux") were considered in the monograph by Hubert and Schäfer [5]. Here, it is important to emphasize that the magnetic vortices are observed predominantly in round tablets, whose height is substantially smaller than their radius, which is also true in regard to the polarization vortices [6]. This circumstance again points to the similarity of the phenomena observed in real systems of small sizes and the phenomena in "mathematically two-dimensional" systems that are studied in the present work.

The specific feature of magnetic systems is that the absolute value of the spontaneous magnetization vector remains unchanged almost for all temperatures below the Curie point. However, this is not the case for the polarization in a ferroelectric. Consequently, in the case of ferroelectrics, it becomes interesting to consider some problems that are not important for ferromagnets, in particular, the distribution of the polarization in the aforementioned vortex immediately after the phase transition [7]. The peculiarity of this distribution, which is worth mentioning here, is the vanishing of the polarization at the center of the vortex. If the cylinder, in which the phase transition occurs, is not continuous solid but has a cylindrical hole (channel) in the center, this vanishing is not the case, although, of course, the polarization near the internal surface is less pronounced than the polarization near the external surface. This can be seen from the polarization distributions obtained numerically. However, we will not pay attention to this circumstance, because it is the less important, the larger is the radius of the hole, which is sufficiently large (approximately 300 nm) in photonic crystals that represent the ultimate goal of our investigations.

If the external surface of the cylinder is metallized, the depolarization field is generated only because of the presence of the internal channel in the system, and the simplest tool to avoid the generation of the depolarization field is also a vortex. For a small radius of the internal channel, this event might not occur; then, a single-domain state is formed, which, however, is not a state with the uniform polarization, because the latter in any case tends to have a zero component normal to the surface of the channel near this surface. The vector field of the polarization as though "wraps around" the channel. The rotation of the polarization vector around the axis of the channel, in this case, occurs in one (for example, clockwise) direction in the vicinity of one semicircle of the contour of the channel surface and in the opposite (counterclockwise) direction in the vicinity of the other semicircle. In contrast to the vortex, this distribution will be referred to as the wrap distribution. The smooth distribution of the polarization in the vicinity of the phase transition point transforms into a domain structure with clearly defined domain walls with an increase in the distance from the phase transition point, because the most energetically favorable are only four directions of polarization and the energy loss due to the unfavorable orientation increases with a decrease in the temperature. It is this domain structure that, in the systems with lattices of channels, is the main subject of our investigation. Therefore, the phenomena occurring in the small-sized systems are of our interest here only to the extent at which they help us to understand what is happening in the large-sized systems.

We begin our investigation with the consideration of an "elementary building block" of a large-sized system, i.e., a square prism with a hole in the center. The ratio of the radius of the channel and the side of the square is the same as for the aforementioned photonic crystals, even though the absolute sizes are significantly smaller because of the computational constraints and our desire at this stage to consider the simplest cases. It should be noted that even the character of the polarization distribution in this simplest system at different temperatures and different boundary conditions sheds some light on what will be observed in the systems with sixteen channels. These systems are already large enough to illustrate, to some extent, the properties of the lattices that are of experimental interest.

The biaxial ferroelectric under consideration is described by the equations of state

$$AP_x + B_1P_x^3 + B_2P_xP_y^2 - G\left[\frac{\partial^2 p_x}{\partial x^2} + \frac{\partial^2 p_x}{\partial y^2}\right] = E_x \quad (4)$$

and by the second similar equation with replacing x by y, and vice versa. We use the coefficients that are close in magnitude to the corresponding coefficients of the $BaTiO_3$ film on the MgO substrate [8], that is,

$$A = A_1(T - T_c) = 7 \times 10^5\ \mathrm{C^{-2}\ m^2\ N},$$

$$B_1 = 20 \times 10^8\ \mathrm{m^5/F\ C^2}, \quad B_2 = -1 \times 10^8\ \mathrm{m^5/F\ C^2},$$

$$G = 6.2 \times 10^{-10}\ \mathrm{m^3/F},$$

but this is done for purposes of illustration and not much else. Therefore, we disregard the higher order terms in the equations of state. In combination with these equations, we use the equations of electrostatics: $\mathrm{div}\,\mathbf{D} = 0$ and $\mathrm{curl}\,\mathbf{E} = 0$. As was already noted, the electric field is considered to be two-dimensional.

In order to perform the numerical calculations, we discretize the differential equations on a lattice with a 0.5×0.5-nm cell. Since the equations of state are nonlinear, we use the Gauss–Seidel iterative method. For this purpose, we start with the "guess" or "initial" values of the polarization components P_x and P_y and the electrical potential ϕ at each lattice site and, consistently considering one or two sites (near the boundaries) in the elementary operation, find corrections to

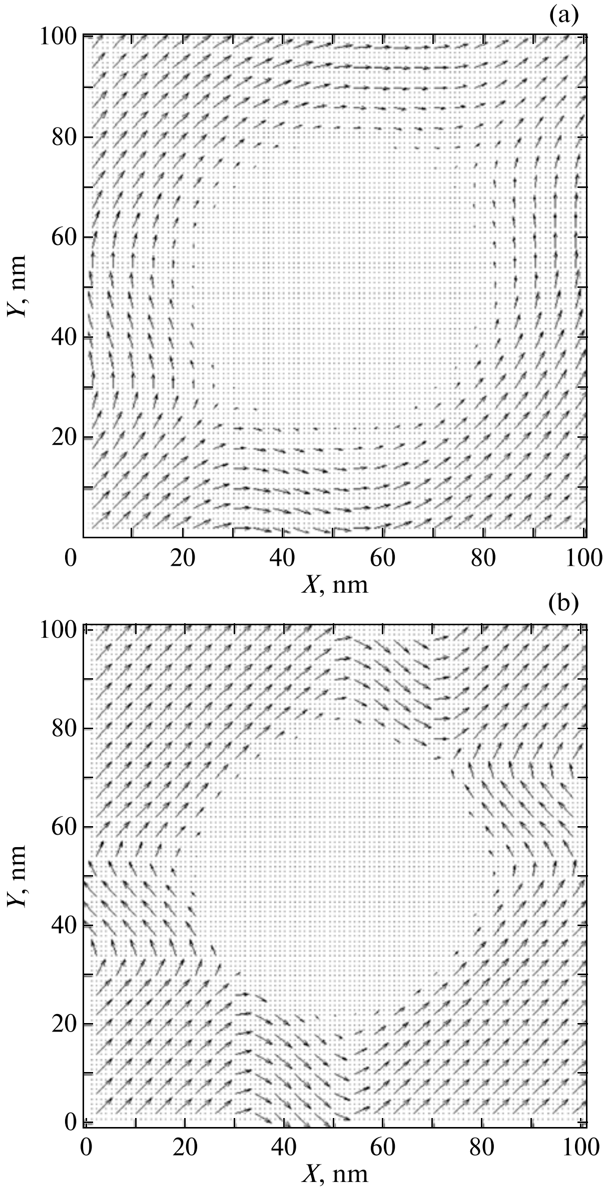

Fig. 1. Vector map of the polarization in an infinite square prism with the central channel and the metallized surface (a) near the phase transition and (b) far from the phase transition. The polar axes are parallel (perpendicular) to the diagonals of the square. In this figure and the figures presented below, the vectors emanate from a small part of the sites of the lattice discretizing the computational problem. The maximum amplitude of the polarization vector is 0.01 C/m^2 near the phase transition and 0.17 C/m^2 far from the phase transition.

these values. The typical number of iterations was 10000; in this case, the typical difference in the values of the polarizations in successive iterations up to this point amounted to approximately 10^{-8} of the quantity itself. We separately stipulate the cases where the number of iterations was different. The boundary conditions for the differential equations have already been mentioned. The numerical calculations have been carried out for two cases: (i) “near the phase transition” at a temperature $T_c - T = 10°C$ and (ii) “far from the phase transition” at a temperature $T_c - T = 150°C$. The starting configuration near the phase transition point was taken as the state with the uniform polarization. The resulting configuration was then used as the initial configuration for simulations far from the phase transition point. We made an attempt to identify the domain structure under the conditions of short-circuited electrodes that were differently oriented with respect to the polar axes. The elucidation of the behavior of the domain structure upon application of an external electric field remained outside the scope of our present work.

3. THE SQUARE PRISM WITH A SINGLE CHANNEL

For the system consisting of a square prism with a single channel, we will consider two types of boundary conditions: (1) the metallized lateral surface of the prism (with a zero electrical potential on all surfaces of the prism), and (2) for all the quantities involved, the periodic boundary conditions that have no direct physical meaning for an isolated square prism. As was already mentioned, the boundaries with a zero electrical potential are considered to be neutral with respect to the polarization; i.e., the derivatives along the normals to the boundaries from both components are equal to zero. Taking into account the periodic conditions, we will attempt to predict the structure in such a square, which enters into the composition of the lattice and is surrounded by other similar squares. We will analyze two types of orientations of the polar axes with respect to the sides of the square.

Let us first consider the case of the polar axes that are parallel (perpendicular) to the diagonals of the square. The distribution of the polarization in the square prism with the metallized surface near the phase transition point is shown in Fig. 1a. Here, there is a distribution of the wrap type with the predominant direction that coincides with one of the directions of the spontaneous polarization. Away from the phase transition point, the general character of the distribution becomes more complex with eight domain walls extending from the hole (Fig. 1b). An even less trivial situation occurs when we set the periodic boundary conditions. The distribution of the polarization near the phase transition point is similar to that described in the previous case (Fig. 2a). This is quite natural because the crystalline anisotropy, which is accounted for by the nonlinear terms of the equations of state, does not affect the distribution of the polarization in the immediate vicinity of the phase transition point. However, the crystalline anisotropy becomes significant far from the phase transition point, which results in the formation of the polarization distribution shown in Fig. 2b. Attention is drawn to the vortex of the

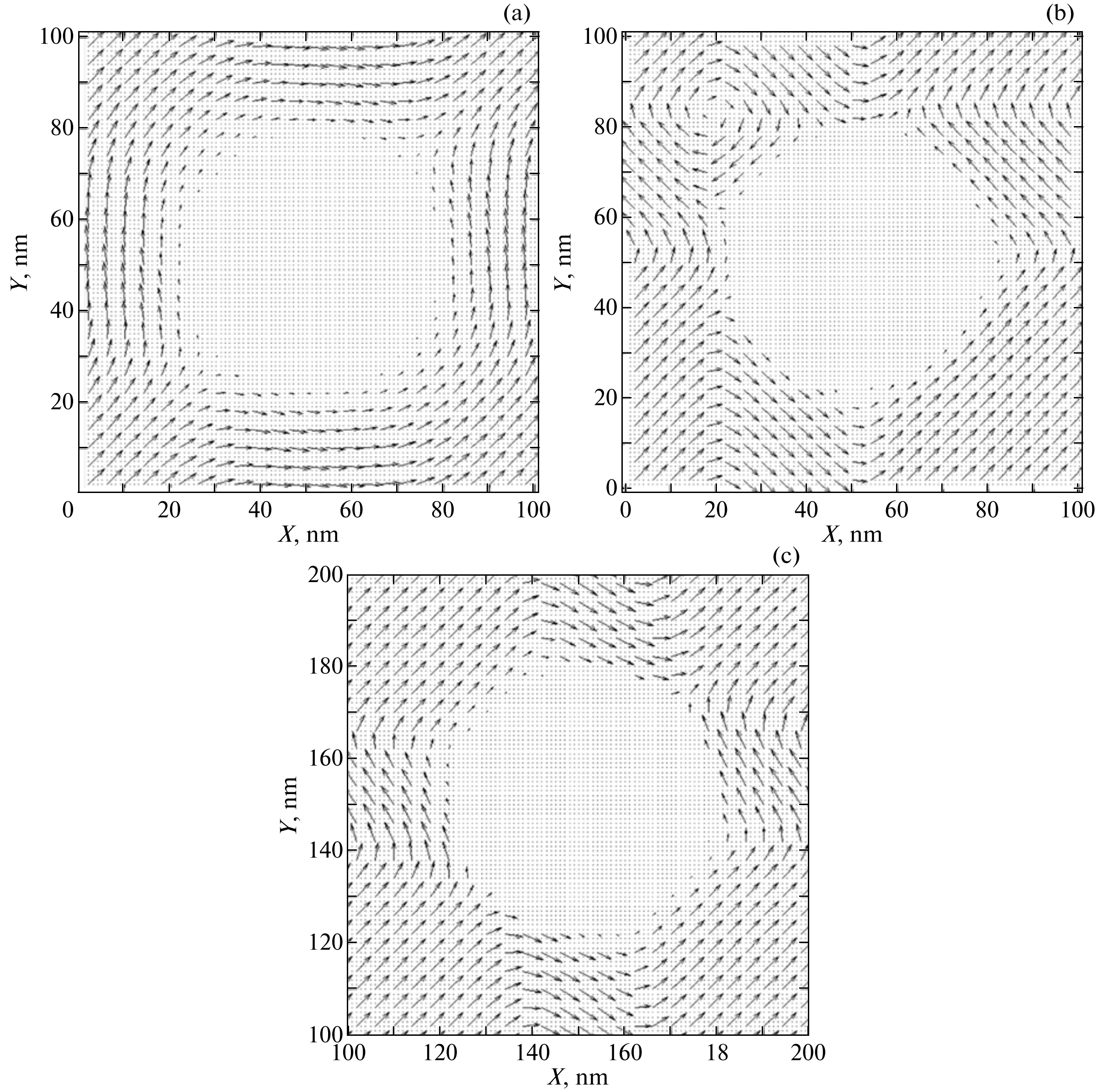

Fig. 2. Vector map of the polarization in an infinite square prism with the central channel under periodic boundary conditions on the surface of the prism (a) near the phase transition and (b) far from the phase transition. (c) The same as in panels (a, b) but for a smaller number of iterations (see the text). The polar axes are parallel (perpendicular) to the diagonals of the square. The maximum amplitude of the polarization vector is 0.01 C/m^2 near the phase transition and 0.17 C/m^2 far from the phase transition.

polarization in the upper left corner of the figure. It is easy to see that we can obtain a different version of the same structure upon the reflection in the plane that lies perpendicular to the plane of the figure and passes through the diagonal of the square, which connects the lower left and upper right corners of the square. Instead of being at the top left of the hole, the vortex will be at the bottom right of the hole, so that the average polarization will remain unchanged. Below, it will be shown that, in the large-sized system (with sixteen channels in our case), there can exist both structures. Another feature of the considered case far from the phase transition point is that, for a smaller number of iterations (1000), there will arise another (also "regular") structure, which contains no vortex and also exists in the system with sixteen holes. This structure is shown in Fig. 2c. It is tempting to interpret this structure as a long-lived nonequilibrium structure; however, within our approach, this conclusion does not have sufficient grounds.

We now turn our attention to the case where the polar axes are parallel (perpendicular) to the sides of the square. The distribution of the polarization in the square prism with the metallized surface near the

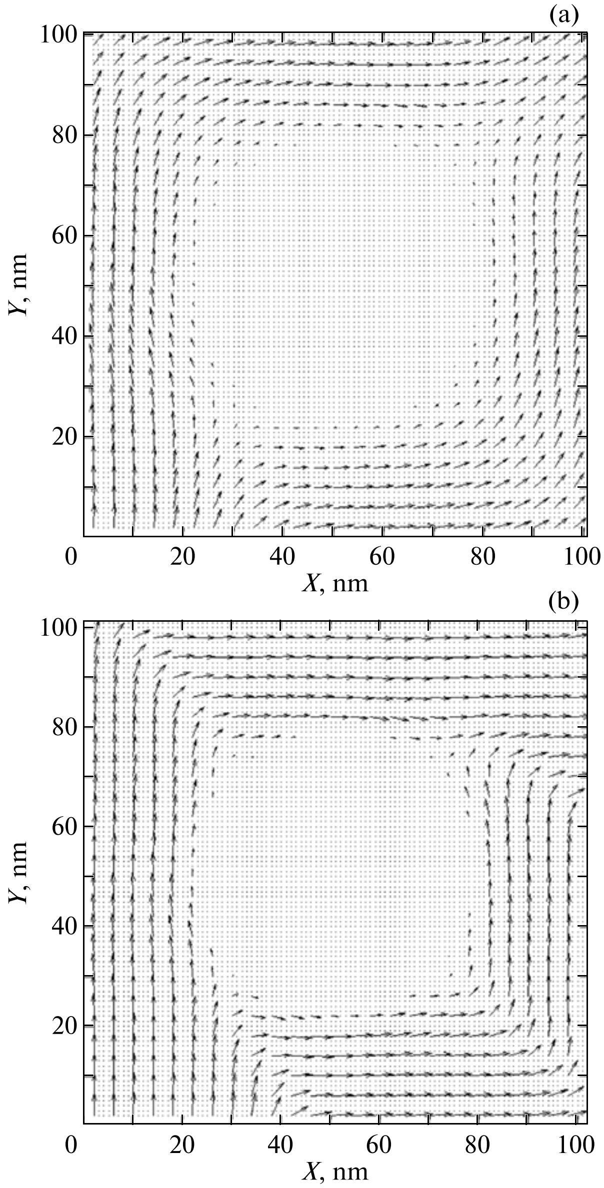

Fig. 3. Vector map of the polarization in an infinite square prism with the central channel and the metallized surface (a) near the phase transition and (b) far from the phase transition. The polar axes are parallel (perpendicular) to the sides of the square. The maximum amplitude of the polarization vector is 0.01 C/m^2 near the phase transition and 0.17 C/m^2 far from the phase transition.

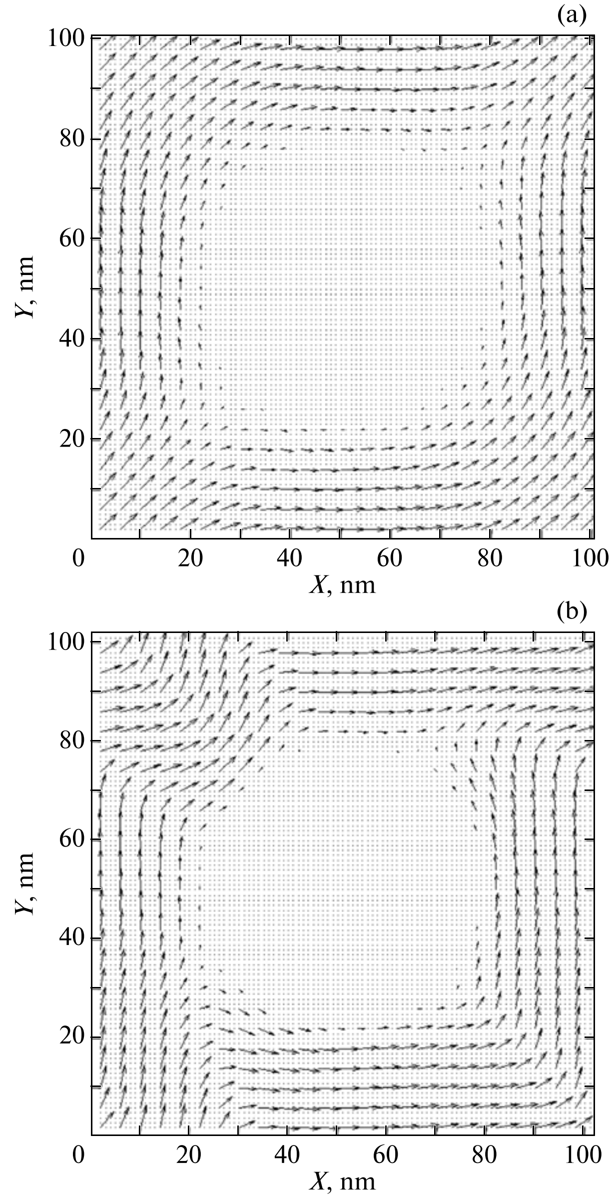

Fig. 4. Vector map of the polarization in an infinite square prism with the central channel under periodic boundary conditions on the surface of the prism (a) near the phase transition and (b) far from the phase transition. The polar axes are parallel (perpendicular) to the sides of the square. The maximum amplitude of the polarization vector is 0.01 C/m^2 near the phase transition and 0.17 C/m^2 far from the phase transition.

phase transition point is shown in Fig. 3a. It can be seen from this figure that the distribution of the polarization near the hole is the distribution of the wrap type. The same type of distribution of the polarization is observed far from the phase transition point (Fig. 3b) with a decreased fraction of the regions with unfavorable polarization. For the periodic boundary conditions, the distributions of the polarization near the phase transition point and far from it are shown in Figs. 4a and 4b, respectively. Here, as in the case of the other orientation, we can obtain a different (equivalent) version of the same structure upon the reflection in the plane that lies perpendicular to the plane of the figure and passes through the diagonal of the square. Similar distributions are also observed in the system with sixteen channels; however, this is not all: the domain structure in a system formed by a large number of channels for the considered orientation of the polar

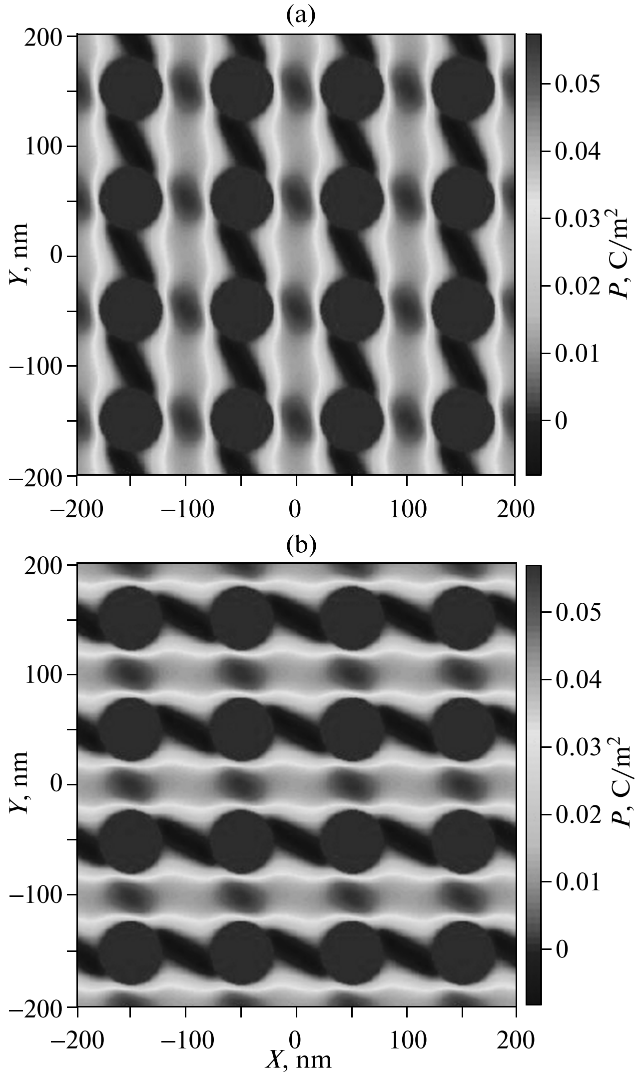

Fig. 5. Distribution of the polarization components in an infinite square prism with sixteen channels near the phase transition. The boundary conditions are periodic. The polar axes coincide with the bisectors of the angles between the coordinate axes. (a) Map of the polarization component along the vertical axis and (b) map of the polarization component along the horizontal axis.

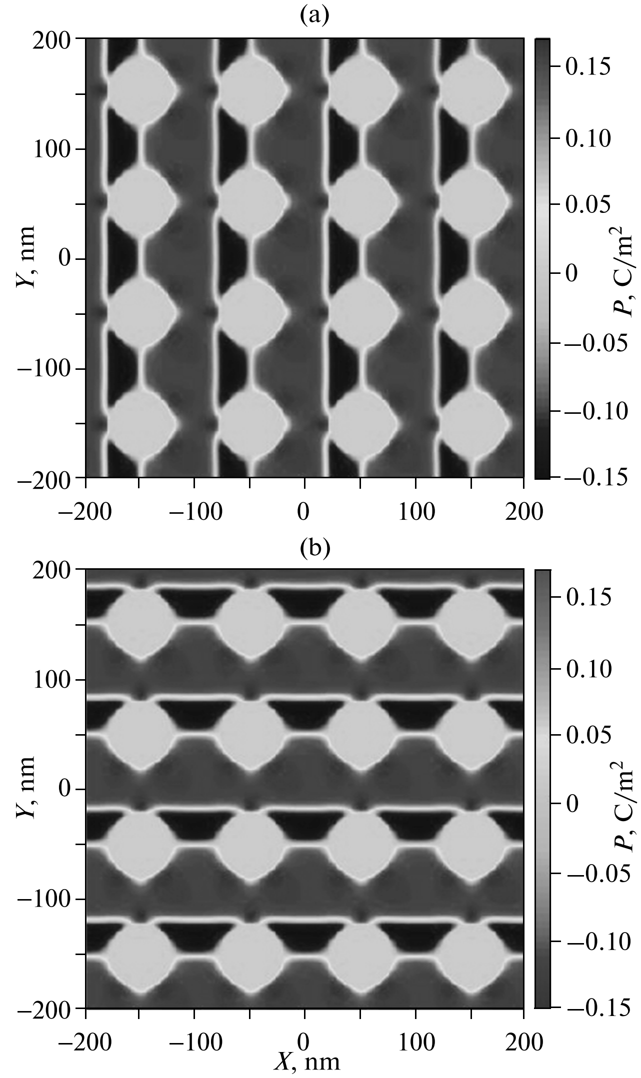

Fig. 6. Distribution of the polarization components in an infinite square prism with sixteen channels far from the phase transition. The boundary conditions are periodic. The polar axes coincide with the bisectors of the angles between the coordinate axes. (a) Map of the polarization component along the vertical axis and (b) map of the polarization component along the horizontal axis.

axes, most likely, is rather complicated, so that the chosen system of sixteen channels is not sufficient to identify it reliably (in contrast to the other orientation of the polar axes).

4. THE RECTANGULAR PRISM WITH MANY CHANNELS

In this section, we will analyze systems that are more closely similar to the experimentally studied systems, namely, films with a regular lattice of channels. More specifically, we have simulated a system of 4 × 4 channels in a square prism. On the surface of the square prism (on the boundaries of the square), we specify two types of boundary conditions. In order to simulate systems with short-circuited electrodes, we set a zero electrical potential (and the neutrality with respect to the polarization) on the horizontal sides of the square and the periodic boundary conditions on the vertical sides of the square. In addition, we use the purely periodic boundary conditions in order to understand the character of the polarization distribution when our system is a part of other considerably larger system.

Let us first consider the case where the polar axes are parallel (perpendicular) to the diagonals of the square. For the periodic boundary conditions and near the phase transition point, the distribution of the

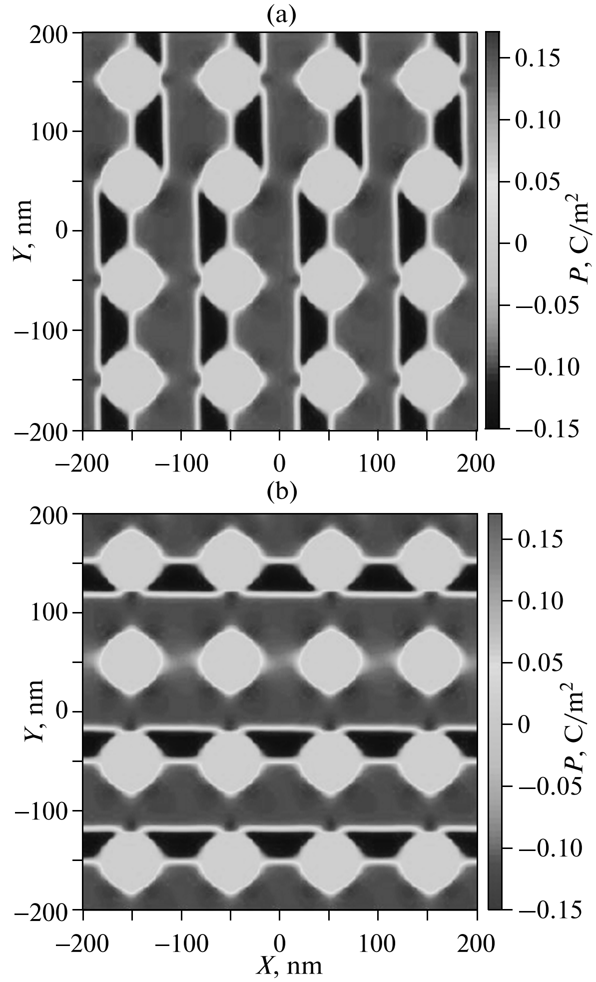

Fig. 7. Distribution of the polarization components in an infinite square prism with sixteen channels far from the phase transition. The boundary conditions are mixed, and the horizontal sides of the square are at a zero electrical potential. The polar axes coincide with the bisectors of the angles between the coordinate axes. (a) Map of the polarization component along the vertical axis and (b) map of the polarization component along the horizontal axis.

polarization is periodic (Fig. 5). Far from the phase transition point, the domain structure is also periodic with a repeating motif that includes one hole (Fig. 6). The distribution of the polarization in a repeating square has the same form as in Fig. 2b. For a smaller number of iterations (1000), the obtained structure is also periodic but different with the polarization distribution in each square, which is shown in Fig. 2c. For the mixed boundary conditions, the distribution of the polarization near the phase transition point is almost the same as in the previous case, with a small modification near the electrodes. In our numerical experiment, this modification was somewhat different for the top and bottom electrodes, which, apparently, led to a significantly different structure as compared to that obtained with the periodic boundary conditions

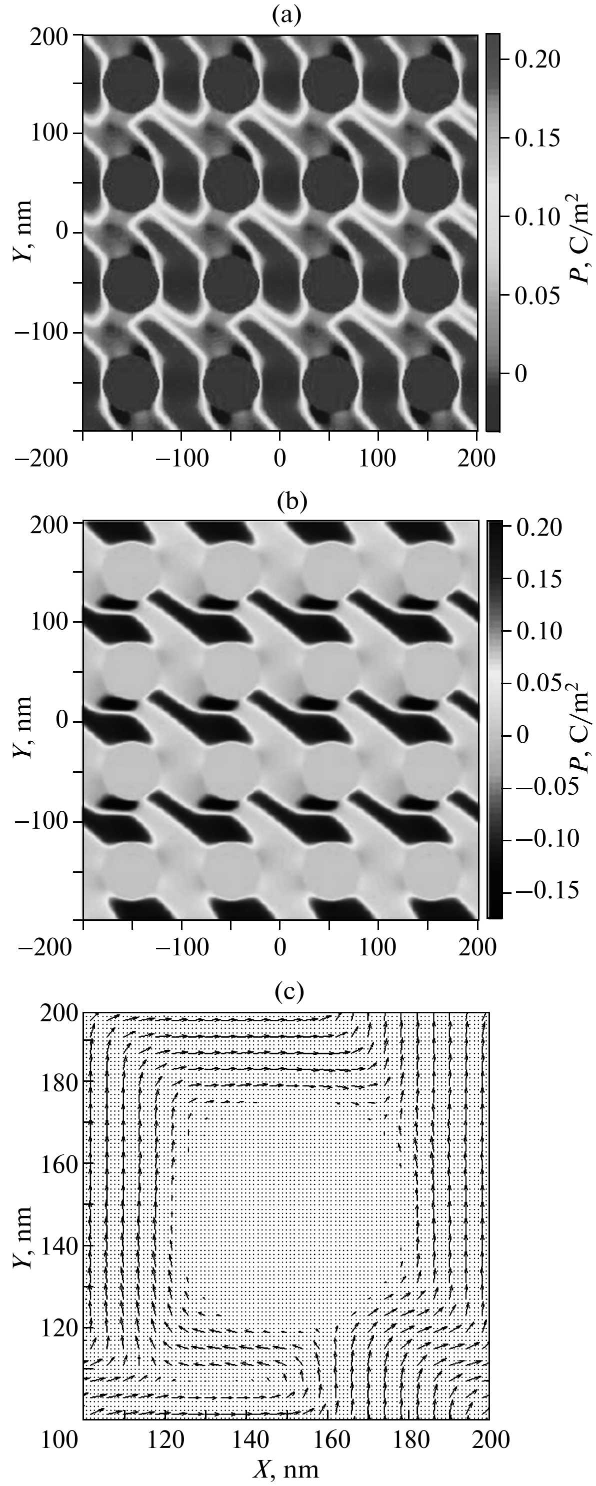

Fig. 8. Distribution of the polarization components in an infinite square prism with sixteen channels far from the phase transition. The boundary conditions are mixed, and the horizontal sides of the square are at a zero electrical potential. The polar axes are parallel (perpendicular) to the sides of the square. (a) Map of the polarization component along the vertical axis, (b) map of the polarization component along the horizontal axis, and (c) vector map of the polarization near one of the internal channels.

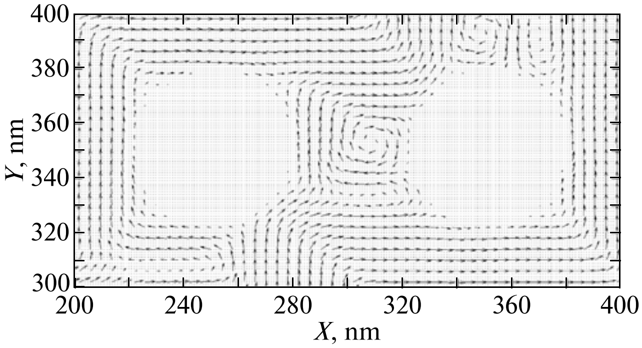

Fig. 9. Vector map of the polarization near the channels at the upper boundary of the square. The boundary conditions are periodic, and the number of iterations is 30000. The polar axes are parallel (perpendicular) to the sides of the square. The maximum amplitude of the polarization vector is 0.17 C/m^2.

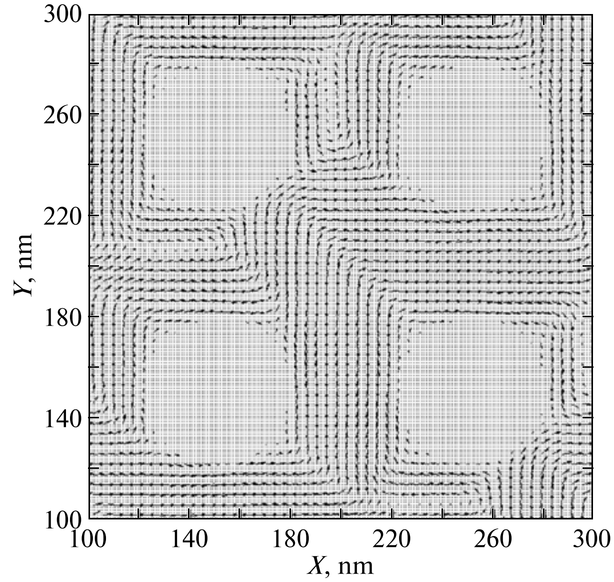

Fig. 10. Vector map of the polarization near the internal channels. The boundary conditions are periodic, and the number of iterations is 30000. The polar axes are parallel (perpendicular) to the sides of the square. The maximum amplitude of the polarization vector is 0.17 C/m^2.

(Fig. 7). This structure can be naturally interpreted as a structure containing two "domains" with a "domain wall" passing through the second (from the top) row of holes. The structure of one of these "domains" (upper row) corresponds to the repetition of the distribution shown in Fig. 2b, while the structure of the other "domain" corresponds to the second version of the distribution (the vortex at the bottom right of the hole) discussed in the previous section.

In the case of the polar axes that are perpendicular (parallel) to the sides of the square, the simplest situation is observed for the mixed boundary conditions; therefore, we first discuss this version. The distribution of the polarization near the phase transition point is very closely similar to the distribution shown in Fig. 5 for the other orientation of the polar axes, which, as was already noted in the previous section, is quite natural. Far from the phase transition point, the obtained structure is almost periodic with the violation of the periodicity near the bottom electrode (Figs. 8a, 8b). The distribution of the polarization near the hole "in depth" is shown in Fig. 8c. It can be seen from this figure that the structure does not contain vortices. The same is also true for the neighborhood of the holes adjacent to the electrodes.

For the periodic boundary conditions, the situation far from the phase transition point is qualitatively different from that described above. Even after 30000 iterations, we could not obtain a regular distribution with a clearly defined periodicity. The distribution of the polarization in the vicinity of the holes near the upper edge of the system contains vortices (Fig. 9). Attention is drawn to the configuration of the system near the four internal holes (Fig. 10). This configuration suggests that the large-sized system tends to be ordered in such a way that its periodicity is $\sqrt{2}$ times larger than the minimum distance between the channels. Such a structure does not contain vortices. They have appeared in our experiment because of the inappropriate method used in order to "cut a piece" with sixteen channels from the large-sized system. With another method of cutting, i.e., for a different orientation of the boundaries of the system with respect to the lines with the minimum distance between the channels, our numerical experiment, quite possibly, could be more successful. However, we could not continue the numerical experiments. It should also be noted that there are substantial differences between the results obtained for the mixed and purely periodic boundary conditions. They suggest that the short-circuited electrodes more significantly affect the domain structure as compared to the case of the other orientation of the polar axes, which has been considered in this work.

5. CONCLUSIONS

The most remarkable result obtained in this work, from our point of view, is the significant difference in the domain structures for two considered orientations of the polar axes with respect to the lattice of channels. Some results indicate that there is an additional influence of the orientation of the electrodes with respect to the lattice of channels; however, the problem, in essence, has not been adequately investigated. We can expect significant differences in the switching and other characteristics for different orientations of the polar axes and electrodes with respect to the lattice, although this assumption should be confirmed by further investigations. The theoretical problem of the domain structure in a biaxial ferroelectric with channels whose axes are perpendicular to the polar plane proved to be complex and has many different aspects, so that the way to solve it is quite long. However, we do not see any other way to understand the properties of switchable photonic crystals based on biaxial ferroelectrics. The present work is only the first step toward in this direction. Of course, the experimental investigations are of great interest, specifically the investigation into the influence of the orientation of the electrodes and the polar axes with respect to the lattice of channels on the properties of photonic crystals. However, at the moment, the results of these investigations are difficult to interpret unambiguously. For example, the lack of the dependence on the orientation in the experiment can mean both the inapplicability of the results of this work to systems with a large number of channels in thin films and the efficiency of the compensation of the depolarization field due to the absorption of ions from the air or due to the other processes occurring on the surface of the channels.

ACKNOWLEDGMENTS

This study was supported by the Russian Foundation for Basic Research, the Ministry of Education and Science of the Russian Federation within the framework of the Russian Federal Targeted Program "Scientific and Scientific–Pedagogical Human Resources for the Innovative Russia in 2009–2013" and the Russian Federal Targeted Program "Research and Development on Priority Directions of the Scientific–Technological Complex of Russia in 2007–2013," and the Center of the Collective Use of Scientific Equipment "Educational and Scientific Association Electronics."

REFERENCES

1. E. Mishina, A. Zaitsev, N. Ilyin, N. Sherstyuk, A. Sigov, Yu. Golovko, V. Muhortov, A. Kolesnikov, Yu. Lozovik, M. Yemtsova, and Th. Rasing, Appl. Phys. Lett. **91** (4), 041107 (2007).
2. E. D. Mishina, N. E. Sherstyuk, A. A. Zaitsev, V. M. Mukhortov, and A. S. Sigov, Bull. Russ. Acad. Sci.: Phys. **71** (10), 1388 (2007).
3. V. M. Mukhortov, Yu. I. Golovko, V. V. Kolesnikov, and S. V. Biryukov, Tech. Phys. Lett. **31** (12), 1029 (2005).
4. D. D. Fong, A. M. Kolpak, J. A. Eastman, S. K. Streifer, P. H. Fuoss, G. B. Stephenson, C. Thomson, D. M. Kim, K. J. Choi, C. B. Eom, I. Grinberg, and A. M. Rappe, Phys. Rev. Lett. **96**, 127601 (2006).
5. A. Hubert and R. Schäfer, *Magnetic Domains: The Analysis of Magnetic Microstructures* (Springer, Berlin, 2009).
6. I. Naumov, L. Bellaiche, and H. Fu, Nature (London) **432**, 737 (2004).
7. A. P. Levanyuk, R. Blinc, and R. Pirc, private communication.
8. N. A. Pertsev, A. G. Zembilgotov, and A. K. Tagantsev, Phys. Rev. Lett. **80**, 1988 (1998).

Translated by O. Borovik-Romanova